

A T Cell Receptor Locus Harbors a Malaria-Specific Immune Response Gene

Natalija Van Braeckel-Budimir,^{1,8} Stephanie Gras,^{2,3,8} Kristin Ladell,^{4,8} Tracy M. Josephs,^{2,3} Lecia Pewe,¹ Stina L. Urban,¹ Kelly L. Miners,⁴ Carine Farenc,³ David A. Price,^{4,5,9,*} Jamie Rossjohn,^{2,3,4,9,*} and John T. Harty^{1,6,7,9,10,*}

¹Department of Microbiology, University of Iowa, Iowa City, IA 52242, USA

²Australian Research Council Centre of Excellence for Advanced Molecular Imaging, Monash University, Clayton, VIC 3800, Australia

³Infection and Immunity Program and Department of Biochemistry and Molecular Biology, Biomedicine Discovery Institute, Monash University, Clayton, VIC 3800, Australia

⁴Division of Infection and Immunity, Cardiff University School of Medicine, Cardiff CF14 4XN, UK

⁵Human Immunology Section, Vaccine Research Center, National Institute of Allergy and Infectious Diseases, NIH, Bethesda, MD 20892, USA

⁶Department of Pathology, University of Iowa, Iowa City, IA 52242, USA

⁷Interdisciplinary Program in Immunology, University of Iowa, Iowa City, IA 52242, USA

⁸These authors contributed equally

⁹Senior author

¹⁰Lead Contact

*Correspondence: priced6@cardiff.ac.uk (D.A.P.), jamie.rossjohn@monash.edu (J.R.), john-harty@uiowa.edu (J.T.H.)

<https://doi.org/10.1016/j.immuni.2017.10.013>

SUMMARY

Immune response (*Ir*) genes, originally proposed by Baruj Benacerraf to explain differential antigen-specific responses in animal models, have become synonymous with the major histocompatibility complex (MHC). We discovered a non-MHC-linked *Ir* gene in a T cell receptor (TCR) locus that was required for CD8⁺ T cell responses to the *Plasmodium berghei* GAP50₄₀₋₄₈ epitope in mice expressing the MHC class I allele H-2D^b. GAP50₄₀₋₄₈-specific CD8⁺ T cell responses emerged from a very large pool of naive Vβ8.1⁺ precursors, which dictated susceptibility to cerebral malaria and conferred protection against recombinant *Listeria monocytogenes* infection. Structural analysis of a prototypical Vβ8.1⁺ TCR-H-2D^b-GAP50₄₀₋₄₈ ternary complex revealed that germline-encoded complementarity-determining region 1β residues present exclusively in the Vβ8.1 segment mediated essential interactions with the GAP50₄₀₋₄₈ peptide. Collectively, these findings demonstrated that *Vβ8.1* functioned as an *Ir* gene that was indispensable for immune reactivity against the malaria GAP50₄₀₋₄₈ epitope.

INTRODUCTION

Genetic regulation of the immune system is a central determinant of health and disease. The observation that random-bred guinea pigs challenged with simple antigens segregate into responder and non-responder groups led to the notion of autosomal-dominant immune response (*Ir*) genes (reviewed in Benacerraf and Germain, 1978). *Ir* genes were first identified as major histocompatibility complex (MHC)-linked (McDevitt

and Chinitz, 1969) and subsequently found to encode specific allotypes of antigen-presenting molecules, such as MHC class II (MHC II) (Benacerraf, 1974; Benacerraf and McDevitt, 1972). Although unidentified at the time, a determinative role was also suggested for the putative T cell receptor (TCR) (Benacerraf and Germain, 1978). MHC II-mediated antigen presentation is required to activate T helper cells and generate antibody responses to T-dependent antigens (Owens and Zeine, 1989). In addition, the host must assemble TCRs capable of engaging specific MHC-peptide (MHCp) complexes with sufficient avidity to trigger immune reactivity (Davis et al., 2003; van der Merwe and Dushek, 2011). Numerous studies of inbred animals have linked the absence of specific immune responses with a lack of appropriate MHC alleles (Marshak et al., 1977; Zinkernagel, 1978). In contrast, despite major advances in our understanding of antigen recognition over the last four decades, it remains unclear whether germline-encoded segments of the TCR can function as *Ir* genes.

CD8⁺ T cells recognize MHC I-restricted peptides via heterodimeric TCRs (Davis and Bjorkman, 1988; Townsend et al., 1985). A vast number of different TCRs can be generated from a limited number of germline-encoded segments through the process of *V(D)J* gene recombination with junctional diversification and subsequent random pairing of the somatically rearranged TCRα and TCRβ chains (Cabaniols et al., 2001; Chothia et al., 1988; Davis and Bjorkman, 1988; Rossjohn et al., 2015; Turner et al., 2006). As a consequence, each individual harbors an extensive repertoire of naive CD8⁺ T cells, which ensures broad recognition of a large number of foreign antigens presented by MHC I (Goldrath and Bevan, 1999). To meet the diversity criterion within space limitations, however, only a few naive precursors are specific for any given epitope (Blattman et al., 2002; Obar et al., 2008), and robust antigen-driven proliferation is required to establish effector and memory CD8⁺ T cell populations (Busch et al., 1998; Goldrath and Bevan, 1999). It is estimated that most naive antigen-specific repertoires in mice do not contain more than 10–300 CD8⁺ T cells (Obar et al., 2008).

Larger pre-immune repertoires comprising 1,000–1,500 naive CD8⁺ T cells have been reported for the murine cytomegalovirus (MCMV) M45₉₈₅₋₉₉₃ and vaccinia virus (VacV) B8R₂₀₋₂₇ epitopes (Jenkins and Moon, 2012), but it remains unclear whether these specific precursor pools define the upper limits of antigen reactivity in the post-thymic landscape of clonotypically distributed TCRs.

Clonal selection ensures the recruitment of biologically and structurally optimal immune receptors from the naive repertoire (Malherbe et al., 2004; Price et al., 2005), frequently leading to biased TCR usage among memory CD8⁺ T cell populations (Miles et al., 2011; Turner et al., 2006). In extreme cases, non-peptidic antigens restricted by non-classical MHC molecules elicit innate-like responses dominated by semi-invariant TCRs (Bendelac et al., 1997; Godfrey et al., 2015; Van Rhijn et al., 2015). Here, we found that a similar phenomenon can regulate conventional CD8⁺ T cell immunity. We demonstrated that an epitope from the *Plasmodium berghei* (*P. berghei*) ANKA glideosome-associated protein (GAP50₄₀₋₄₈), a key pathogenic target in experimental cerebral malaria (ECM), was associated with the largest naive CD8⁺ T cell repertoire yet described in laboratory mice (Jenkins and Moon, 2012). We also revealed the molecular properties of these GAP50₄₀₋₄₈-specific TCRs, demonstrating exclusive use of the Vβ8.1 segment underpinned by direct interactions with the malarial peptide. Mice lacking Vβ8.1 did not respond to the GAP50₄₀₋₄₈ epitope after *P. berghei* infection and did not develop ECM. Moreover, the very large pool of naive precursors conferred enhanced control of primary infection with recombinant *Listeria monocytogenes* (*L. monocytogenes*) expressing the GAP50₄₀₋₄₈ epitope. Collectively, these findings extend the notion of *Ir* genes to incorporate germline-encoded components of antigen-specific TCRs.

RESULTS

GAP50₄₀₋₄₈-Specific CD8⁺ T Cells Exhibit an Extreme TCR Bias

ECM in susceptible C57BL/6 (B6) mice infected with *P. berghei* ANKA (Engwerda et al., 2005) is a valuable model of severe malarial disease (Brewster et al., 1990). It is established that the development of ECM is critically dependent on pathogenic CD8⁺ T cells (Amani et al., 2000; Haque et al., 2011; Yañez et al., 1996) expressing Vβ8⁺ TCRs (Boubou et al., 1999; Mariotti-Ferrandiz et al., 2016), especially those specific for the H-2D^b-restricted GAP50₄₀₋₄₈ epitope (Howland et al., 2013). However, it is not known why GAP50₄₀₋₄₈-specific CD8⁺ T cells are pathogenic in ECM. To address this issue, we set out to generate TCR retrogenic mice harboring monoclonal or oligoclonal CD8⁺ T cell populations specific for individual epitopes derived from *P. berghei*, namely thrombospondin-related adhesion protein (TRAP)₁₃₀₋₁₃₈, sporozoite-specific protein 20 (S20)₃₁₈₋₃₂₆, and GAP50₄₀₋₄₈ (Holst et al., 2006; Hafalla et al., 2013; Howland et al., 2013). As a first step, we immunized three separate groups of B6 mice with peptide-pulsed dendritic cells (DCs) followed 7 days later by recombinant *L. monocytogenes* (LM) expressing the same epitope. This accelerated prime-boost approach (Badovinac et al., 2005) elicited large CD8⁺ T cell responses specific for TRAP₁₃₀₋₁₃₈, S20₃₁₈₋₃₂₆, and GAP50₄₀₋₄₈ (Figure S1A). We then used the corresponding MHC I tetramers and a panel of

anti-mouse Vβ antibodies to profile the constituent malaria-specific TCRs.

CD8⁺ T cells specific for TRAP₁₃₀₋₁₃₈ and S20₃₁₈₋₃₂₆ expressed several different TCR Vβ segments with distinct preferences (Figures 1A and S1B). For example, almost 75% of the S20₃₁₈₋₃₂₆-specific repertoire was focused on Vβ8.1/8.2 and Vβ8.3, while the TRAP₁₃₀₋₁₃₈-specific repertoire was dominated by Vβ2 and Vβ7. In contrast, >99% of GAP50₄₀₋₄₈-specific CD8⁺ T cells expressed Vβ8.1/8.2, which cannot be discriminated by antibody staining (Figures 1A and S1B). These segments comprised <15% of the corresponding GAP50₄₀₋₄₈ tetramer[−] repertoires in the same mice (Figure 1B). Moreover, an identical TCR bias was observed after inoculation of sporozoites by mosquito bite or immunization with radiation-attenuated sporozoites or DC-GAP50₄₀₋₄₈ alone (data not shown), and similar results were obtained with other strains of mice expressing the MHC I allele H-2D^b, including CB6F1 and BALB.b (Figure S1C). The GAP50₄₀₋₄₈ epitope therefore mobilized an almost exclusive repertoire of TCR Vβ-defined memory CD8⁺ T cells.

To gain a deeper understanding of this extreme bias, we sorted GAP50₄₀₋₄₈-specific CD8⁺ T cells directly *ex vivo* from DC-LM-GAP50₄₀₋₄₈-immunized B6 mice and performed an unbiased molecular analysis of all expressed *TRA* and *TRB* gene rearrangements (Quigley et al., 2011). Sequence analysis showed that >98% of transcripts encoded Vβ8.1 (Figure 1C and Table S1). In contrast, a variety of *TRAV* gene segments were detected, indicating promiscuous pairing of diverse TCRα chains with a constrained repertoire of Vβ8.1⁺ TCRβ chains (Figure 1D). Almost 40% of retrogenic T cells generated with a GAP50₄₀₋₄₈-specific TCRβ chain bound the GAP50₄₀₋₄₈ tetramer in naive mice, while only ~1% of retrogenic T cells generated with a TRAP₁₃₀₋₁₃₈-specific TCRβ chain bound the TRAP₁₃₀₋₁₃₈ tetramer (Figure S2). These data suggested that the Vβ8.1 segment was a major recognition element for GAP50₄₀₋₄₈-specific CD8⁺ T cells.

Analysis of the third TCRβ chain complementarity-determining region (CDR3β) revealed additional features of the GAP50₄₀₋₄₈-specific repertoire (Figures S3A–S3C, Table S1). In particular, we identified a common CDR3β length (~60% of translated sequences incorporated 14 amino acids) (Figure S3A), an almost uniform bias toward *TRBD2* gene usage within a single reading frame (Figure S3B), and a strong preference for *TRBJ* gene segments from the Jβ2 cluster (Figure S3C). Moreover, the Vβ-Dβ junction lacked N additions, and a germline-encoded CDR3β motif (¹⁰⁴CASSDWG¹¹⁰) was present in >95% of sequences (Table S1 and Figure 1E). These data demonstrated that a highly convergent pattern of gene rearrangements effectively “licensed” the Vβ8.1-driven immune response to the GAP50₄₀₋₄₈ epitope (Quigley et al., 2010).

The C-Terminal Region of the GAP50₄₀₋₄₈ Peptide Is a “Hotspot” for TCR Recognition

To understand the molecular basis of this extreme TCR bias, we first determined the structure of the H-2D^b-GAP50₄₀₋₄₈ complex at a resolution of 2.2 Å (Table S2). The bound peptide adopted a canonical extended conformation (Young et al., 1994), with four solvent-exposed amino acid residues (P4-L, where L is leucine; P6-A, where A is alanine; P7-K, where K is lysine; and P8-Y,

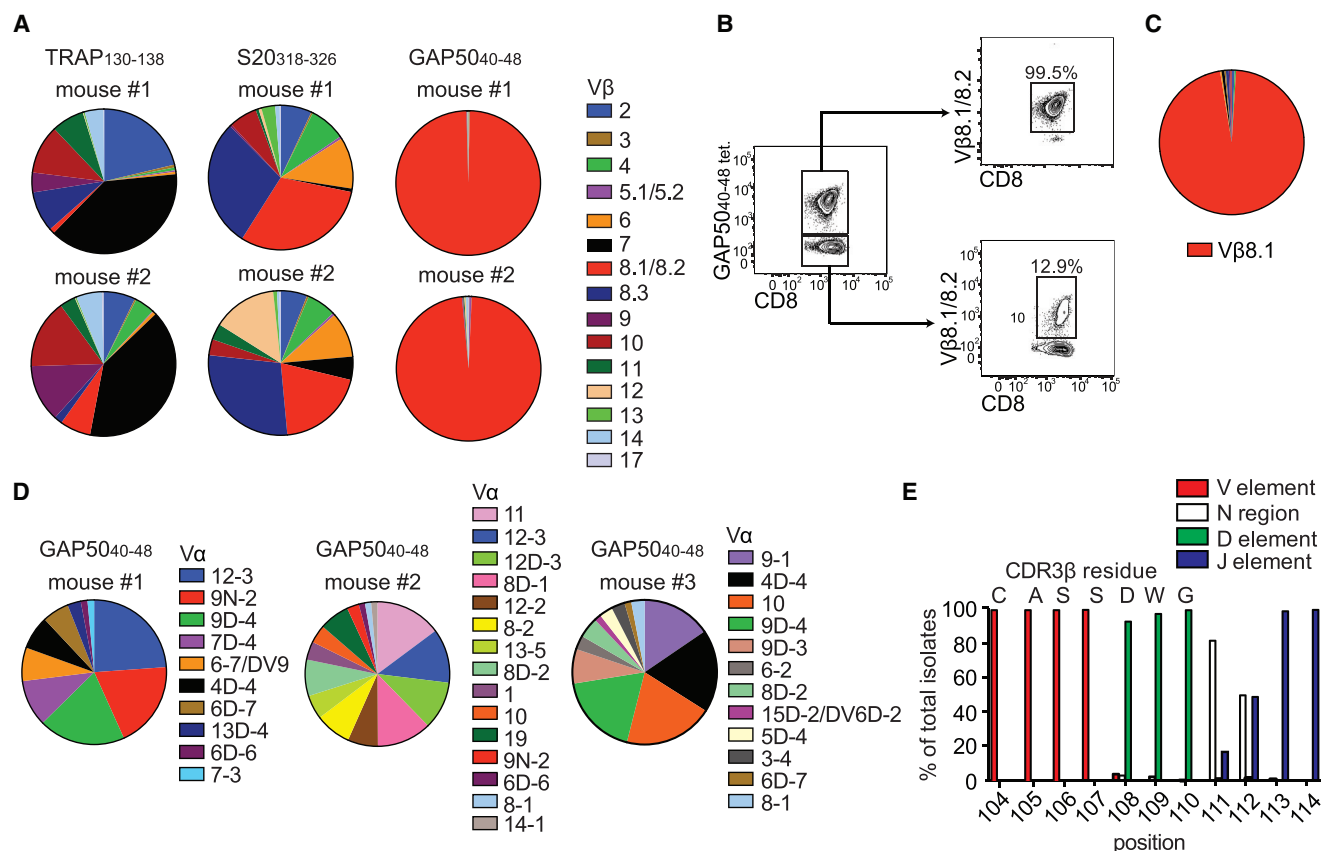


Figure 1. GAP50₄₀₋₄₈-Specific CD8⁺ T Cells Express Biased TCRs

(A and B) Mice were primed with peptide-coated DCs and boosted on day 7 with recombinant *L. monocytogenes* expressing the same epitope.

(A) The TCR Vβ repertoire was assessed using splenocytes isolated from immunized mice by staining with the indicated tetramers and Vβ-specific antibodies. Results are shown for two mice for each antigen specificity. Data represent four independent experiments (n = 5 mice/group). Cumulative data are shown in Figure S1B.

(B) Extreme focusing of the GAP50₄₀₋₄₈-specific repertoire does not reflect the overall frequency of Vβ8.1/8.2⁺ clonotypes in the CD8⁺ T cell compartment. Data represent three independent experiments (n = 4–5 mice/group).

(C and D) Confirmation of TCR bias at the transcriptional level. Sequences were derived from GAP50₄₀₋₄₈-specific CD8⁺ T cells isolated from the spleens of mice previously immunized with DC-LM-GAP50₄₀₋₄₈ (total = 316 molecular clones).

(C) Population-level analysis revealed an extreme bias toward Vβ8.1.

(D) TCR Vα sequence distributions from three different mice are depicted. No obvious bias was apparent in the Vα repertoire.

(E) Origin of CDR3β amino acids expressed relative to the total number of molecular Vβ8.1⁺ clones (n = 5 mice). Vβ, red; Dβ, green; Jβ, purple; N segments, white. See also Figures S1–S3 and Table S1.

where Y is tyrosine) representing potential contacts for the TCR (Figure 2A).

To determine which GAP50₄₀₋₄₈ residues were important for TCR recognition, we replaced individual amino acids with alanine (Ala), except for the wild-type (WT) Ala residue at position 6 (P6), which was replaced with serine (Ser) (Figure 2B). We did not mutate the critical H-2D^b anchor residues at P5 or P9 (Valkenburg et al., 2013). The WT and mutant peptides were then used at saturating concentrations in intracellular cytokine staining assays to determine the impact of each residue on the functional reactivity of GAP50₄₀₋₄₈-specific CD8⁺ T cells (Figures 2C and S4). Interferon-γ (IFN-γ) production relative to the WT peptide was unaffected by the substitutions at P1, P2, and P3 (Figure 2C). In contrast, the mutations at P4-L and P6-A diminished IFN-γ production, while the mutations at P7-K and P8-Y abolished IFN-γ production (Figure 2C). The C-terminal P7-K and

P8-Y residues were therefore crucial for GAP50₄₀₋₄₈-specific CD8⁺ T cell activation and represented “hotspots” for TCR engagement (Figure 2D).

GAP50₄₀₋₄₈ Peptide “Hotspots” Interact Exclusively with the TCRβ Chain

Next, we determined the structure of a prototypical Vβ8.1⁺ TCR, derived from the GAP50₄₀₋₄₈-specific CD8⁺ T cell clone NB1 (Table S3), in complex with H-2D^b-GAP50₄₀₋₄₈ (Figure 3A, Table S2). The NB1 TCR docked centrally atop the H-2D^b cleft, with an angle of 43° and a buried surface area (BSA) of approximately 2,200 Å², values that fall within the range previously determined for TCR-MHCp complexes (Figure 3B; Rossjohn et al., 2015). All six CDR loops were involved to a varying extent in the interaction with H-2D^b-GAP50₄₀₋₄₈ (Figure 3C). Namely, the CDR3α and CDR3β loops contributed 24% and 20% of the

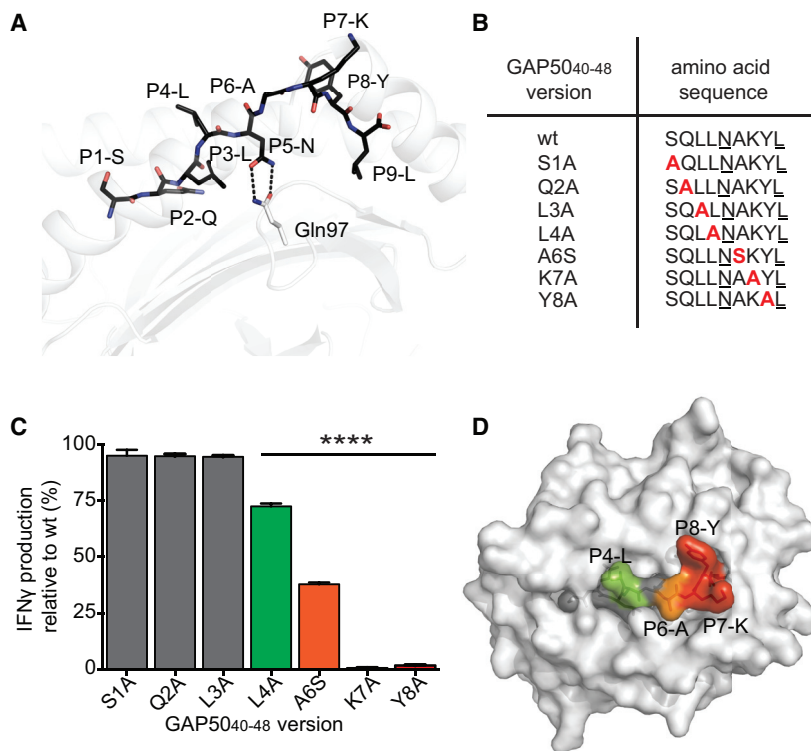


Figure 2. TCR Interactions Focus on the C-Terminal Region of the GAP50₄₀₋₄₈ Peptide

(A) The structure of the GAP50₄₀₋₄₈ peptide in complex with H-2D^b. The GAP50₄₀₋₄₈ peptide is represented as black sticks in the antigen-binding cleft of H-2D^b (white cartoon). The P2-Q and P9-L anchor residues are buried within the antigen-binding cleft, and P5-N acts as a secondary anchor residue forming hydrogen bonds (black dashes) with Gln97 (white stick) at the base of the antigen-binding cleft of H-2D^b (white cartoon).

(B) A panel of peptide mutants was generated by replacing amino acids with Ala or Ser at selected positions (red). Anchor residues are underlined.

(C) Splenocytes isolated from GAP50₄₀₋₄₈-immunized mice were restimulated for 5 hr *in vitro* using WT or mutant peptides. The production of IFN- γ induced by stimulation with the different mutant peptides is expressed relative to the production of IFN- γ induced by stimulation with the WT peptide. Data represent two independent experiments performed in triplicate. Bars represent mean \pm SD. Significance was assessed using a one-way ANOVA (*****p* < 0.0001).

(D) The effect of peptide substitutions on recognition of the H-2D^b-GAP50₄₀₋₄₈ complex by specific CD8⁺ T cell clones. The surface of H-2D^b is shown in white. Peptide residues that were not mutated or did not affect IFN- γ production are shown in gray. Green represents up to a 25% decrease in T cell activation; orange represents up to a 70% decrease in T cell activation; red represents a total abrogation of T cell activation.

See also Figure S4 and Table S2.

BSA, respectively, while the CDR1 α and CDR2 α loops each contributed \sim 17% of the BSA (Figure 3C). Somewhat unexpectedly given the extreme TCR V β bias, the germline-encoded CDR1 β and CDR2 β loops each contributed only \sim 10% of the BSA. Thus, the cumulative β chain contribution to the overall BSA was substantially smaller (39%) relative to the cumulative α chain contribution (61%) (Figure 3C). However, >95% of TCR-GAP50₄₀₋₄₈ peptide interactions were mediated by the TCR β chain (Figure 3D, Table S4), while the TCR α chain primarily contacted the MHC molecule (74% of the BSA) (Figure 3E, Table S4).

The CDR1 α loop stretched between the peptide-binding α helices of H-2D^b, with tyrosine (Tyr) 28 α playing a principal role by contacting glutamic acid (Glu) 163, Glu166, and tryptophan (Trp) 167 at the N-terminal end of the cleft (Figure 3F, Table S4). The CDR2 α loop sat above the α 2 helix, with arginine (Arg) 57 α lying flat above residues Glu154 and Ala158 (Figure 3G). The CDR3 α loop contacted a large stretch of the α 1 helix (spanning residues 58–72), with hydrophobic and hydrogen bond contacts exclusively mediated by germline-encoded residues from the J α segment (¹⁰⁸YAQ¹¹⁰, where Q is glutamine) (Figure 3H). The NB1 TCR α chain engaged the H-2D^b molecule with a large footprint over the N-terminal region of the antigen-binding cleft (Figure 3B). Mutational analyses of H-2D^b binding performed using three distinct GAP50₄₀₋₄₈-specific CD8⁺ T cell clones further indicated that different V β 8.1⁺ TCRs used an identical MHC I docking strategy (Figure S5, Table S5).

Interactions between the NB1 TCR α chain and the GAP50₄₀₋₄₈ peptide were limited to two van der Waals interactions between the CDR3 α loop and P4-L (Table S4). In contrast, the NB1 TCR V β 8.1 region dominated contacts with the bound epitope (44 of 46 contacts) (Table S4). Moreover, all three CDR β loops contacted the C terminus of the peptide (P6–8) (Figures 3I–3K), encompassing the previously identified “hotspots” for CD8⁺ T cell recognition (Figure 2D). The CDR1 β loop interacted with both P7-K and P8-Y via its ²⁸N-DY³¹ motif (where N is asparagine and D is aspartic acid). More specifically, P7-K and P8-Y formed a notch in which aspartic acid (Asp) 30 β was inserted as a peg, forming a salt bridge with P7-K (Figure 3J). In addition, asparagine (Asn) 28 β hydrogen bonded via its main chain with P7-K, while the aromatic group of Tyr31 β sat above P8-Y (Figure 3J). Contacts were also established between P8-Y and the CDR2 β loop via Tyr57. Accordingly, P8-Y was closely sequestered upon TCR binding (Figure 3J). The conserved CDR3 β motif ¹⁰⁸DW¹⁰⁹ (where W is tryptophan), which was most frequently germline-encoded within the D gene (Figure 1E), interacted with P6-A and P7-K (Figure 3K). The large Trp109 β side chain lay flat on top of P6-A, acting as a lid covering the central part of the epitope, while Asp108 β and P7-K formed a salt bridge (Figure 3K).

TCR β chain interactions with the H-2D^b molecule were modest in comparison to the TCR α chain (Table S4). The CDR1 β loop contacted only glutamine (Gln) 72 via Tyr31 β (Figures 3I and 3J). The side chains of valine (Val) 58 β from the CDR2 β loop abutted Val76 from H-2D^b, establishing an interaction

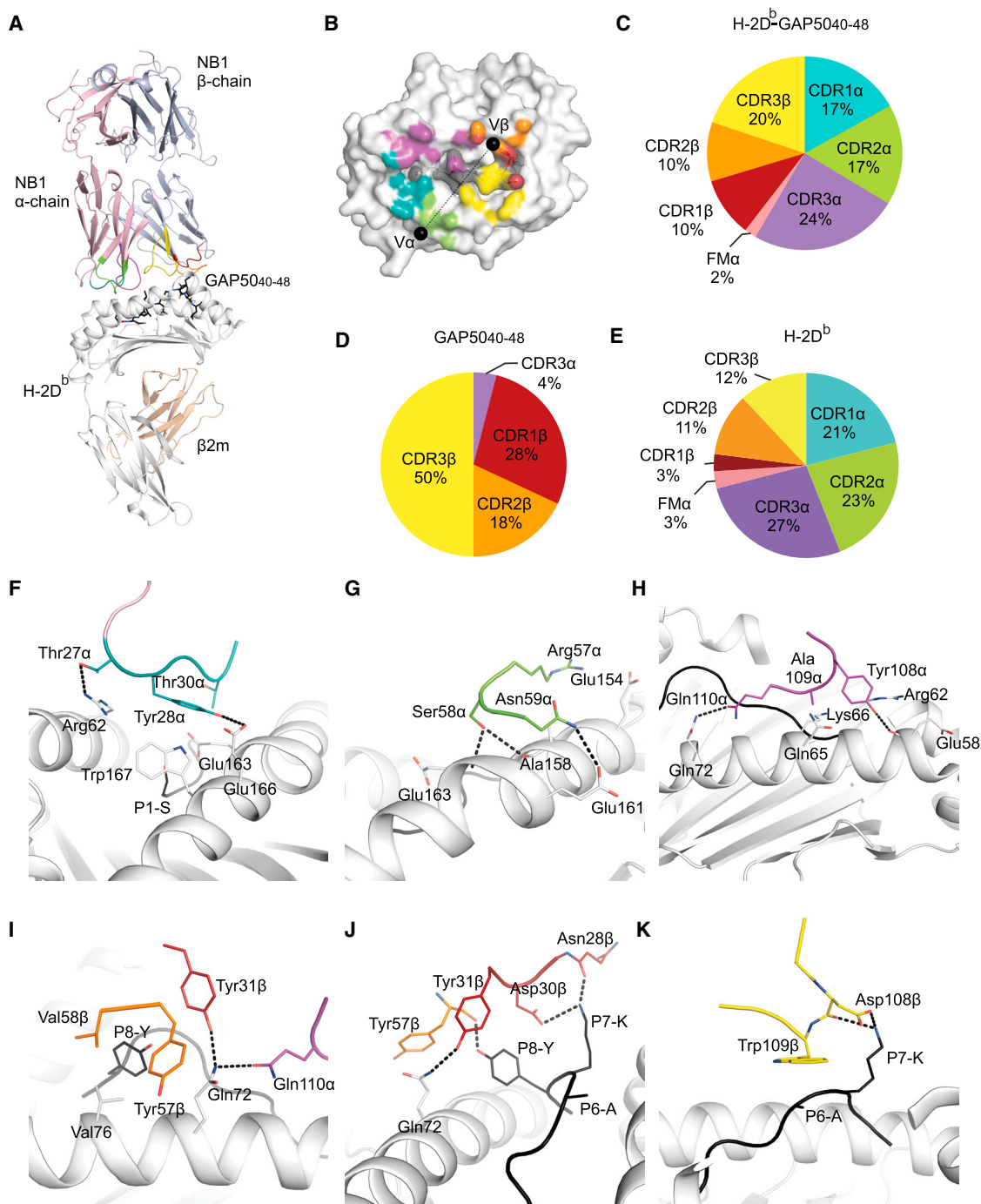


Figure 3. GAP50₄₀₋₄₈-Specific TCR Bias Is Peptide Driven

(A) The crystal structure of the NB1 TCR (α chain, pink cartoon; β chain, purple cartoon) bound to the GAP50₄₀₋₄₈ peptide (black sticks) presented by H-2D^b (heavy chain, white cartoon; β 2m, wheat cartoon).

(B) The CDR loop contribution to the BSA is represented as teal (CDR1 α), green (CDR2 α), purple (CDR3 α), red (CDR1 β), orange (CDR2 β), or yellow (CDR3 β). Black spheres represent the center of mass for the V α and V β .

(C–E) The contribution (%) of the CDR loops to the interaction with H-2D^b-GAP50₄₀₋₄₈ (C), GAP50₄₀₋₄₈ (D), and H-2D^b (E).

(F–K) Contact residues between H-2D^b-GAP50₄₀₋₄₈ and CDR1 α (F), CDR2 α (G), CDR3 α (H), CDR1 β (I, J), CDR2 β (J), and CDR3 β (K). The CDR color scheme is maintained. Residues that make contacts with the GAP50₄₀₋₄₈ peptide or H-2D^b (white) are depicted as black and white sticks, respectively. The H-2D^b molecule is represented as white cartoon, and hydrogen bonds are shown as black dashes.

See also [Figure S5](#) and [Tables S2–S5](#).

network extended by Tyr57 β -mediated contacts with Gln72, Arg75, and Val76. The conserved CDR3 β ¹⁰⁸DW¹⁰⁹ motif from the *TRBD2* gene segment formed interactions with the hinge region of the α 2 helix, whereby Trp109 β nestled between histidine (His) 155 and Ser150. Thus, germline-encoded TCR β chain residues played a minor role in contacting the H-2D^b molecule.

The observation that the prototypical NB1 TCR interacted with GAP50₄₀₋₄₈ extensively via its β chain suggested that the peptide itself drove the extreme bias toward V β 8.1. This notion contrasts with prevailing dogma, which asserts that germline bias arises as a consequence of allotype-specific MHC reactivity (Garcia et al., 2009).

CDR1 Residues Unique to V β 8.1 Are Critical for GAP50₄₀₋₄₈ Peptide Recognition

These structural insights allowed us to identify candidate factors underlying the exclusive recruitment of V β 8.1⁺ TCR clonotypes into the immune repertoire. To determine the precise amino acid sequences involved in this process, we initially focused on the germline-encoded CDR1 β and CDR2 β loops. Sequence alignments revealed that the CDR1 β loops encoded by six *TRBV* genes shared a common Asp30 β , while the Asp30 β -Tyr31 β motif was unique to V β 8.1. In the other five *TRBV* genes, Tyr31 β was replaced by a smaller threonine (Thr)/Ser residue (Table S6A). Three *TRBV* genes shared a common Val58 β residue in the encoded CDR2 β loop, but only V β 8.1 incorporated the additional Tyr57 β required to sequester P8-Y (Table S6B).

Although the conserved CDR3 β region interacted with both the peptide and H-2D^b, we wanted to determine whether the germline-encoded V β 8.1 residues were essential for TCR-mediated recognition of H-2D^b-GAP50₄₀₋₄₈. We therefore conducted affinity measurement studies using targeted mutants of the NB1 TCR. Ala mutagenesis was performed on residues Asp30 β and Tyr31 β in the CDR1 β loop and residues Tyr57 β and Val58 β in the CDR2 β loop (Figures 4A and 4B). In addition, Tyr31 β was mutated to Thr to mimic the CDR1 β loop encoded by the five other *TRBV* genes that shared Asp30 β (Figures 4A and 4B). Affinity values for each TCR mutant, measured by surface plasmon resonance (SPR), were compared with the affinity of the WT TCR. The results showed that mutations in the CDR2 β loop exerted a moderate effect, decreasing binding affinity by 3-fold compared with the NB1 TCR (Figures 4A and 4B). In contrast, mutation of Tyr31 β to either Ala or Thr in the CDR1 β loop substantially reduced binding to H-2D^b-GAP50₄₀₋₄₈, resulting in $K_{d,eq}$ values >200 μ M (Figures 4A and 4B). As shown in Figure 3I and Table S4, Tyr31 β contacted both H-2D^b and P8-Y. Additionally, mutation of Asp30 β to Ala abolished binding to H-2D^b-GAP50₄₀₋₄₈ (Figures 4A and 4B). The Asp30 β residue contacted the peptide alone via a salt bridge with P7-K, one of the two defined “hotspot” residues for TCR recognition (Figure 3J and Table S4).

The unique germline-encoded CDR1 β ³⁰DY³¹ motif within the V β 8.1 segment therefore underpinned both the extreme TCR bias and the residue-specific patterns of epitope recognition that characterized the CD8⁺ T cell response to H-2D^b-GAP50₄₀₋₄₈.

The Naive GAP50₄₀₋₄₈-Specific CD8⁺ T Cell Repertoire Is Extraordinarily Large

Extreme TCR focusing described in the literature appears to result primarily from the selection of high-affinity clonotypes

during repeated or persistent infection (Busch and Pamer, 1999; Malherbe et al., 2004; Price et al., 2005; Savage et al., 1999), but recombinatorial bias and structural constraints dictate the available pre-immune repertoire (Miles et al., 2011; Neller et al., 2015; Turner et al., 2006). We therefore adapted a tetramer-based enrichment protocol (Moon et al., 2007) to enumerate the naive repertoires specific for the *P. berghei* epitopes TRAP₁₃₀₋₁₃₈, S20₃₁₈₋₃₂₆, and GAP50₄₀₋₄₈. Parallel experiments were performed with tetramers representing epitopes derived from ovalbumin (H-2K^b-OVA₂₅₇₋₂₆₄) and lymphocytic choriomeningitis virus glycoprotein (H-2D^b-LCMV GP₃₃₋₄₁) to allow comparison with previously reported evaluations of the naive antigen-specific T cell repertoire (Jenkins and Moon, 2012).

Precursor numbers specific for OVA₂₅₇₋₂₆₄ and GP₃₃₋₄₁ were consistent with prior reports (183 \pm 33 and 358 \pm 40 cells, respectively) (Figure 5A; Jenkins and Moon, 2012). The naive S20₃₁₈₋₃₂₆-specific repertoire was relatively small (\sim 79 \pm 19 cells), while fewer than 10 cells were counted in the TRAP₁₃₀₋₁₃₈-specific repertoire (Figure 5A). In contrast, as described recently (Gordon et al., 2015), the GAP50₄₀₋₄₈-specific naive repertoire was extraordinarily large (2,935 \pm 305 cells; Figure 5A). The upper limit for a naive antigen-specific CD8⁺ T cell repertoire in mice was previously established at 1,200–1,500 cells for the MCMV M45₉₈₅₋₉₉₃ and VacV B8R₂₀₋₂₇ epitopes (Jenkins and Moon, 2012). The GAP50₄₀₋₄₈-specific repertoire therefore constituted the largest naive antigen-specific CD8⁺ T cell pool yet described (Figure 5B). Moreover, >99% of naive GAP50₄₀₋₄₈-specific CD8⁺ T cells expressed V β 8.1 (Figure 5A). These findings indicated that the extreme TCR V β bias observed in the memory CD8⁺ T cell pool did not evolve as a consequence of repertoire focusing in response to antigenic challenge, but instead reflected intrinsic recognition of the GAP50₄₀₋₄₈ epitope characterized by absolute dependence on the interaction with V β 8.1.

Phenotypically, the GAP50₄₀₋₄₈-specific precursors resembled classical naive CD8⁺ T cells, comprised of a large CD44^{lo} population (>90%) and a small CD44^{hi} “virtual memory” population (<10%) akin to OT-I and P14 TCR-Tg cells from naive mice (Figure 5C; Akue et al., 2012). Expression of the CD5 surface protein, which acts as a surrogate marker for the strength of TCR activation induced by self-derived MHCp complexes during thymic selection and frequently correlates with T cell avidity for antigen (Fulton et al., 2015; Mandl et al., 2013), was uniformly higher on naive GAP50₄₀₋₄₈-specific CD8⁺ T cells compared with the majority of non-GAP50₄₀₋₄₈-specific naive CD8⁺ T cells in the same host and mirrored levels expressed by OT-I cells, which bear high-affinity TCRs (Figure 5D; Kedl et al., 2000). These data suggested that the extremely large pool of V β 8.1⁺ precursors specific for the GAP50₄₀₋₄₈ epitope arose as a consequence of strong thymic selection.

Absence of V β 8.1 Compromises the GAP50₄₀₋₄₈-Specific CD8⁺ T Cell Response

The results of our structural and mutagenesis studies indicated that immune responses to GAP50₄₀₋₄₈ required the presence of V β 8.1. To test this hypothesis, we studied the generation of GAP50₄₀₋₄₈-specific CD8⁺ T cell responses in C57/L (H-2^b)

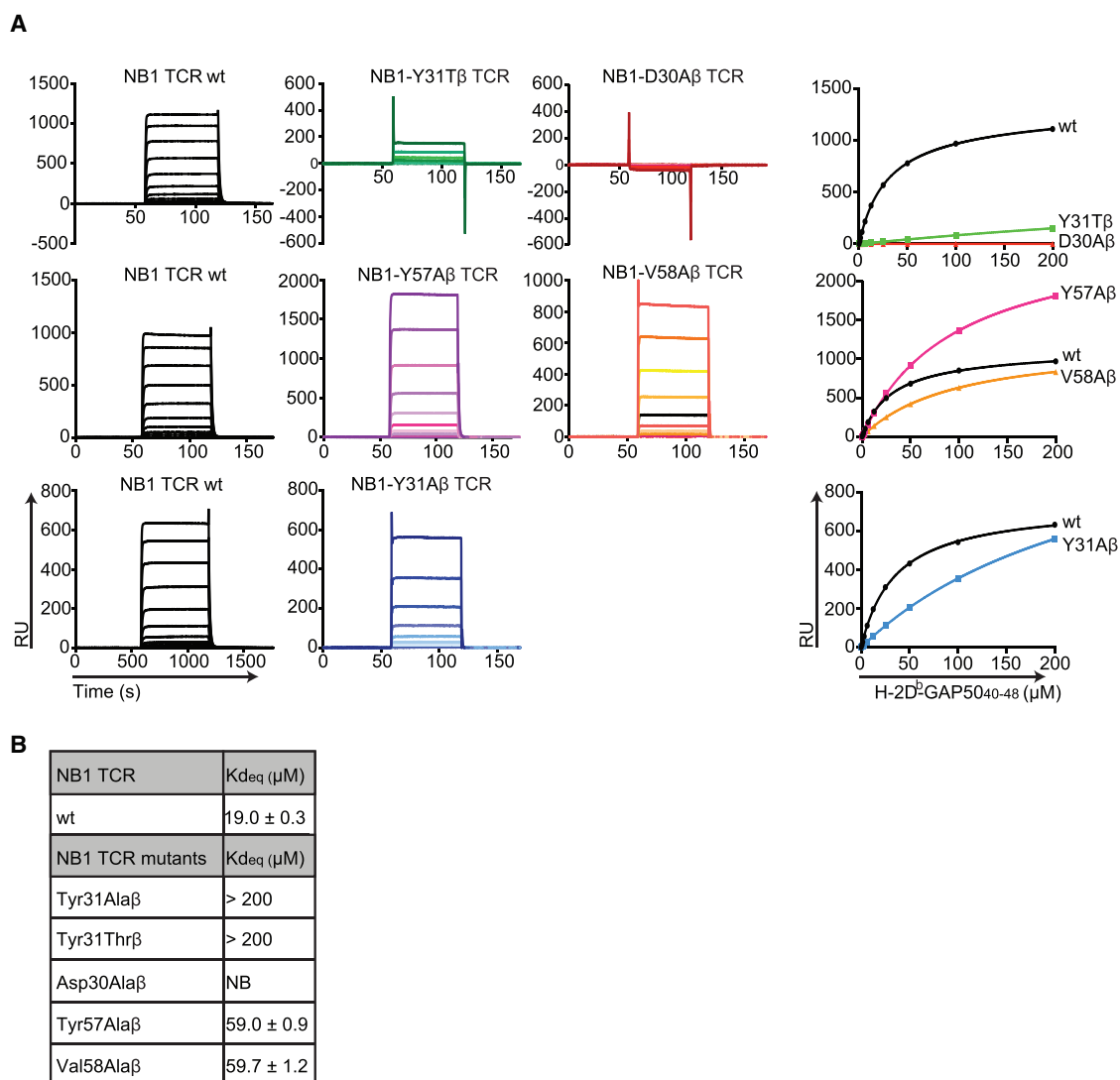


Figure 4. Binding Affinities of NB1 TCR Mutants for H-2D^b-GAP50₄₀₋₄₈

(A) Surface plasmon resonance (SPR) analysis of NB1 WT (black) and the indicated mutant (colored) TCRs across a range of H-2D^b-GAP50₄₀₋₄₈ concentrations up to a maximum of 200 μM. Representative SPR binding curves are shown for the NB1 WT TCR (black) and NB1 mutant TCRs with the following β chain substitutions: Y31A (green), D30A (red), Y57A (pink), V58A (orange), and Y31A (blue). Each NB1 mutant TCR was tested in parallel with the NB1 WT TCR.

(B) Summary table representing equilibrium binding affinities of NB1 TCR mutants for H-2D^b-GAP50₄₀₋₄₈. NB, no binding; RU, response units. Data represent two independent experiments performed in duplicate (mean ± SEM).

See also Tables S6A and S6B.

mice, which lack Vβ8 (Behlke et al., 1986). For this purpose, C57/L mice and control B6 mice were exposed to infection with 10³ *P. berghei* ANKA sporozoites, a challenge that induces ECM in susceptible mouse strains.

In contrast to B6 mice, which generated GAP50₄₀₋₄₈-specific responses comprising 45% of the total CD8⁺ T cell pool in peripheral blood and >10% of the total CD8⁺ T cell pool in the brain by day 7 after infection, the GAP50₄₀₋₄₈-specific response in C57/L mice was undetectable in both compartments (Figures 6A and 6B). This finding strongly suggested that the GAP50₄₀₋₄₈-specific CD8⁺ T cell response was critically dependent on Vβ8.1. In addition, B6 × C57/L F1 mice mounted substantial Vβ8.1⁺ GAP50₄₀₋₄₈-specific CD8⁺ T cell responses after infec-

tion with LM-GAP50₄₀₋₄₈ or *P. berghei* ANKA (data not shown), excluding negative selection of GAP50₄₀₋₄₈-specific naive precursors in C57/L mice. However, C57/L mice lack other Vβ genes (Vβ5, Vβ8, Vβ9, Vβ11, and Vβ12) (Behlke et al., 1986), which could potentially compromise the ability to mount alternative responses to GAP50₄₀₋₄₈. Countering this argument, the magnitude of the total *P. berghei*-specific CD8⁺ T cell response, as detected by the frequency of CD8⁺ T cells expressing surrogate activation markers (CD11a^{hi}CD8^{lo}) (Rai et al., 2009) at day 7 after infection, was essentially identical in B6 and C57/L mice (Figure 6C). Moreover, C57/L mice did not develop ECM. Instead, these mice survived beyond day 9 after infection and succumbed to high-level parasitemia after ~3 weeks (Figure 6D). Thus, Vβ8.1 was

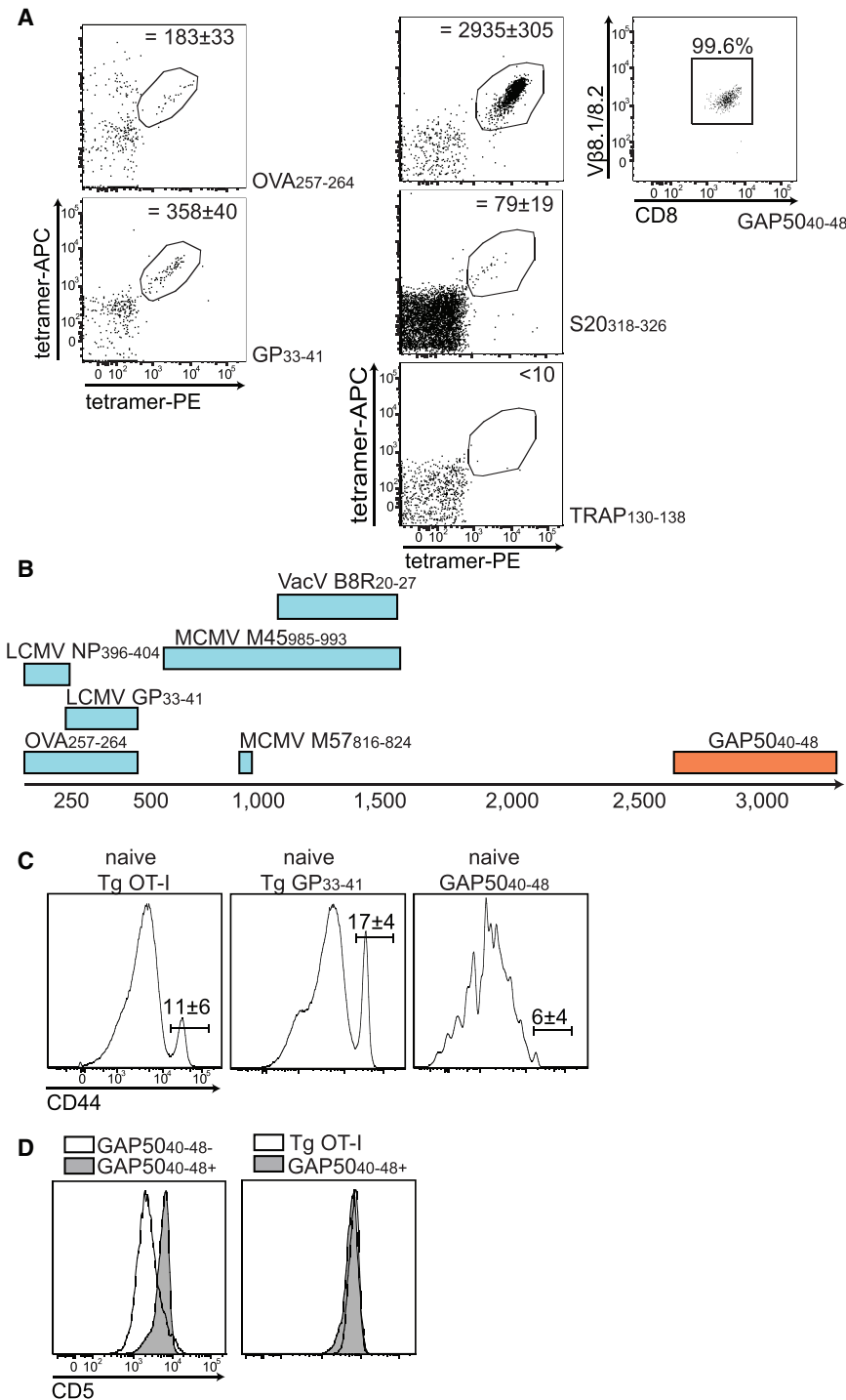


Figure 5. The Naive GAP50₄₀₋₄₈-Specific CD8⁺ T Cell Repertoire Is Extremely Large

(A) CD8⁺ T cells specific for OVA₂₅₇₋₂₆₄, GP₃₃₋₄₁, GAP50₄₀₋₄₈, S20₃₁₈₋₃₂₆, and TRAP₁₃₀₋₁₃₈ were enriched from the spleens and macroscopic lymph nodes of naive C57BL/6 mice and used to calculate the final numbers of tetramer⁺ cells indicated in each plot. Target cells were identified as CD8⁺CD90.2⁺CD11b⁻CD11c⁻B220⁻tetramer(APC)⁺tetramer(PE)⁺. Depicted numbers of naive precursors were calculated as mean ± SD from 11 mice for the GAP50₄₀₋₄₈-specific repertoire. Right panel: Vβ8.1/8.2 expression on naive GAP50₄₀₋₄₈-specific CD8⁺ T cells.

(B) Sizes of the naive repertoires specific for various CD8⁺ T cell epitopes. The number of naive GAP50₄₀₋₄₈-specific precursors is represented as a range from 2,700–3,250 cells (total n = 11 mice).

(C and D) Phenotypic characterization of naive GAP50₄₀₋₄₈-specific CD8⁺ T cells.

(C) Expression of CD44 on naive GAP50₄₀₋₄₈-specific CD8⁺ T cells was compared with CD8⁺ T cells obtained from naive Tg OT-I and P14 mice.

(D) Expression of CD5 on naive GAP50₄₀₋₄₈-specific CD8⁺ T cells was compared with total naive, non-GAP50₄₀₋₄₈-specific CD8⁺ T cells (left) and with naive Tg OT-I cells (right). Data represent two independent experiments (n = 4 mice/group). Bars depict mean ± SD.

GAP50₄₀₋₄₈-specific CD8⁺ T cells in the brain could lead to eventual rupture of the blood-brain barrier, which triggers well-recognized neurological symptoms leading to rapid death (7–9 days after infection) (Howland et al., 2013). In contrast to susceptible B6 mice, which all succumbed to ECM by day 7 after infection with *P. berghei* ANKA-parasitized red blood cells (pRBCs), only 20% of CB6F1 mice succumbed to ECM (Figure 6E). We therefore considered the possibility that a strain-specific difference in the size of the naive GAP50₄₀₋₄₈-specific CD8⁺ T cell repertoire might underlie these differential outcomes. Tetramer pull-down of naive GAP50₄₀₋₄₈-specific CD8⁺ T cells revealed that CB6F1 mice harbored ~3-fold fewer precursors than B6 mice (Figure 6F). Moreover, this smaller naive pool resulted in a

necessary for the generation of detectable GAP50₄₀₋₄₈-specific CD8⁺ T cell responses and the development of ECM.

GAP50₄₀₋₄₈-Specific CD8⁺ T Cells Are Pathogenic in ECM

A recent publication suggested that GAP50₄₀₋₄₈-specific CD8⁺ T cells play a key role in the pathogenesis of ECM in susceptible B6 mice (Howland et al., 2013). Mechanistically, accumulation of

smaller GAP50₄₀₋₄₈-specific CD8⁺ T cell response in CB6F1 mice compared with B6 mice at day 6 after infection with *P. berghei* ANKA pRBCs (Figure 6G). These results suggested that a GAP50₄₀₋₄₈-specific CD8⁺ T cell response threshold might be required for the induction of ECM. To confirm a threshold-dependent pathogenic role for GAP50₄₀₋₄₈-specific CD8⁺ T cells in ECM, we generated a large GAP50₄₀₋₄₈-specific CD8⁺ T cell response in CB6F1 or B6 mice prior to infection with *P. berghei* ANKA. We observed no meaningful difference in the

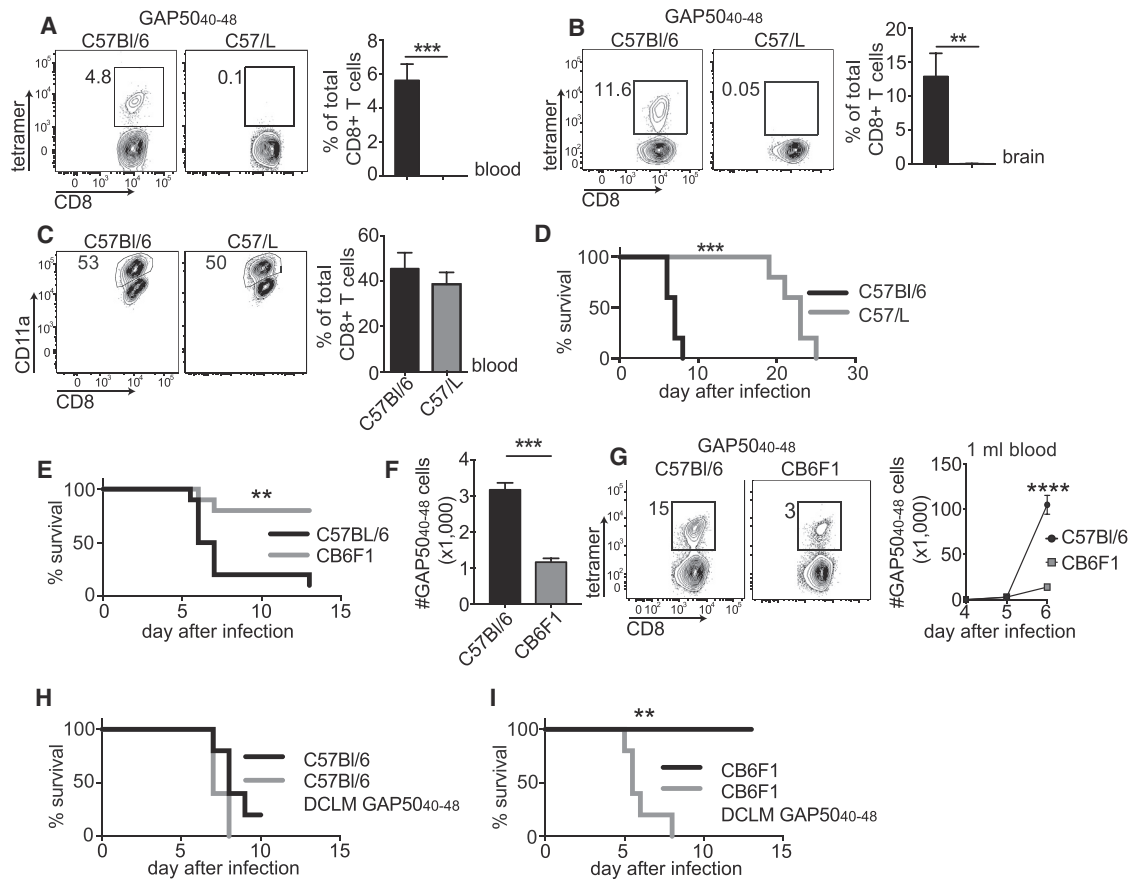


Figure 6. V β 8.1 Is Required for the Generation of GAP50₄₀₋₄₈-Specific CD8⁺ T Cells and the Development of ECM

(A and B) C57BL/6 and C57/L mice were infected with 10^3 *P. berghei* ANKA sporozoites. H-2D^b-GAP50₄₀₋₄₈ tetramer⁺ cells were quantified in the blood (A) and brains (B) at day 7 post-infection (representative plots: left; summary graph: right).

(C) Magnitude of the activated CD8⁺ T cell response at day 7 post-infection, expressed as percent CD11a^{hi}CD8^{lo} of total CD8⁺ T cells (representative plots: left; summary graph: right). Naive control values were subtracted from individual values. Data represent two independent experiments ($n = 3$ mice/group). Bars depict mean \pm SD. Significance was assessed using an unpaired, two-tailed t test (** $p < 0.01$, *** $p < 0.001$).

(D) Survival curves for C57BL/6 mice and C57/L mice after infection with *P. berghei* ANKA. Data represent three independent experiments ($n = 5$ mice/group). Significance was assessed using the Mantel-Cox log rank test (*** $p = 0.001$).

(E) C57BL/6 and CB6F1 mice were infected with 10^6 *P. berghei*-parasitized red blood cells (pRBCs). Mice were monitored for the development of ECM symptoms and scored for survival over a period of 2 weeks. Data represent three independent experiments ($n = 5$ mice/group). Significance was assessed using the Mantel-Cox log rank test (** $p = 0.0025$).

(F) GAP50₄₀₋₄₈-specific CD8⁺ T cells were tetramer-enriched from naive C57BL/6 and CB6F1 mice and quantified to estimate repertoire size. Cumulative results are shown from two independent experiments (total $n = 4$ mice/group). Bars depict mean \pm SEM. Significance was assessed using an unpaired, two-tailed t test (*** $p < 0.001$).

(G) C57BL/6 and CB6F1 mice were infected with 10^6 pRBCs. The GAP50₄₀₋₄₈-specific CD8⁺ T cell response was followed in the blood of infected mice using H-2D^b-GAP50₄₀₋₄₈ tetramers. All C57BL/6 mice succumbed to ECM by days 6 and 7, while all CB6F1 mice survived. Data represent two independent experiments ($n = 5$ mice/group). Bars depict mean \pm SD. Significance was assessed using an unpaired, two-tailed t test (**** $p < 0.0001$).

(H and I) C57BL/6 and CB6F1 mice were injected i.v. with 5×10^5 GAP50₄₀₋₄₈ peptide-coated DCs and then infected 7 days later with recombinant attenuated LM-GAP50₄₀₋₄₈. At a memory time point after LM infection, DC-LM-GAP50₄₀₋₄₈-immunized or non-immunized mice were infected with 10^6 pRBCs. Survival curves are shown for C57BL/6 mice (H) and CB6F1 mice (I). Data represent two independent experiments ($n = 5$ mice/group). Significance was assessed using the Mantel-Cox log rank test ($p = 0.0993$ in H; ** $p = 0.0018$ in I).

onset of ECM symptoms or the mortality rate between previously immunized and non-immunized B6 mice, demonstrating that sufficient numbers of GAP50₄₀₋₄₈-specific effector CD8⁺ T cells can be generated from the large pool of naive precursors in this susceptible strain (Figure 6H). In contrast, prior immunization against GAP50₄₀₋₄₈ was required to render all CB6F1 mice susceptible to ECM after *P. berghei* ANKA infection (Figure 6I). Collectively, these findings demonstrated that a numerical

threshold delimited the pathogenicity of GAP50₄₀₋₄₈-specific CD8⁺ T cells in the etiology of ECM.

GAP50₄₀₋₄₈-Specific CD8⁺ T Cells Protect against LM-GAP50₄₀₋₄₈

Although pathogenic in the context of ECM, we hypothesized that the rapid generation of a substantial GAP50₄₀₋₄₈-specific response from the large number of naive precursors may protect

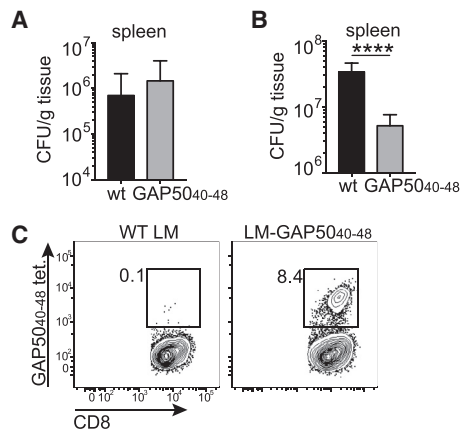


Figure 7. Large Numbers of GAP50₄₀₋₄₈-Specific CD8⁺ T Cells Control Primary *L. monocytogenes* Infection

(A) BALB/c mice were infected i.v. with 5×10^3 CFU of WT LM or recombinant LM-GAP50₄₀₋₄₈. Bacterial burden was measured in the spleen on day 5. Data represent two independent experiments ($n = 4$ mice/group). Bars depict mean \pm SD.

(B) C57BL/6 mice were infected i.v. with 10^4 CFU of WT LM or recombinant LM-GAP50₄₀₋₄₈. Bacterial burden was measured in the spleen on day 5. Cumulative results are shown from three independent experiments (total $n = 14$ – 15 mice/group). Bars depict mean \pm SEM. Significance was assessed using an unpaired, two-tailed t test (**** $p < 0.0001$).

(C) Representative flow cytometry plots showing H-2D^b-GAP50₄₀₋₄₈ tetramer staining of splenocytes isolated from infected C57BL/6 mice at day 5 post-infection.

against infection controlled primarily by CD8⁺ T cells. To address this possibility, we determined whether B6 mice could better control primary infection with virulent LM-GAP50₄₀₋₄₈ compared with virulent WT LM.

To ensure comparability, we first established that the two different strains of LM exhibited similar virulence in the absence of a GAP50₄₀₋₄₈-specific CD8⁺ T cell response. For this purpose, we infected BALB/c mice (H-2^d), which were non-responsive to the H-2D^b-restricted GAP50₄₀₋₄₈ epitope (Figure 7A). Bacterial burden assessed in the spleens of infected mice 5 days after infection with 5×10^3 colony-forming units (CFU) of each strain was similar between the two groups, suggesting equivalent virulence *in vivo* (Figure 7B). In contrast, we measured ~ 10 -fold fewer bacteria in the spleens of LM-GAP50₄₀₋₄₈-infected B6 mice compared with WT LM-infected B6 mice (Figures 7C and 7D). This superior control of bacterial infection in LM-GAP50₄₀₋₄₈-infected B6 mice was accompanied by a large GAP50₄₀₋₄₈-specific response, comprising $>8\%$ of the total CD8⁺ T cell pool in the spleen (Figure 7E). The expansion of GAP50₄₀₋₄₈-specific effector cells from a large pool of naive precursors therefore conferred protection in the context of an infection controlled by CD8⁺ T cells.

DISCUSSION

Conceptual frameworks developed in the 1970s, prior to a detailed understanding of the molecular interactions that govern T cell antigen recognition, established the notion of genetically controlled immune responsiveness. Overwhelming experimental data have since accumulated to validate one original proposition

that MHC-linked *Ir* genes dictate the presentation of specific antigens in immunogenic form (Benacerraf and Germain, 1978). There is also some evidence to support the idea that germline-encoded components of the TCR interact preferentially with defined MHC allotypes (Garcia et al., 2009; Scott-Browne et al., 2009), building on the earlier theoretical work of Niels Jerne (Jerne, 1971). However, it has not been shown previously that heritable elements of an antigen receptor can license immune reactivity, a scenario postulated almost four decades ago as an alternative model to explain the *Ir* gene phenomenon (Benacerraf and Germain, 1978). In this study, we demonstrated that CD8⁺ T cell responses specific for the murine malaria epitope GAP50₄₀₋₄₈ were entirely dependent on amino acid residues unique to the TCR V β 8.1 segment, thereby providing insights into the genetic mechanisms that control adaptive immunity.

As a consequence of structural constraints focused primarily on the CDR1 β loop, both naive and antigen-expanded H-2D^b-restricted GAP50₄₀₋₄₈-specific CD8⁺ T cells almost invariably express V β 8.1⁺ TCRs. Similarly extreme biases are typically associated with innate-like responses to non-peptidic antigens presented by non-classical MHC molecules, although immune reactivity among these unconventional T cell subsets is generally endowed by a conserved TCR α chain (Van Rhijn et al., 2015). Narrow TCR repertoires specific for peptide epitopes have previously been linked with low numbers of naive precursors (Moon et al., 2007) and clonal selection during the genesis of memory populations, especially in the presence of constant or repetitive antigen stimulation (Busch and Pamer, 1999; Price et al., 2005; Savage et al., 1999). Paradoxically, the pre-immune GAP50₄₀₋₄₈-specific repertoire was the largest yet described in mice, numbering $\sim 3,000$ cells in a naive B6 host. Moreover, this substantial precursor pool did not seem to arise as a consequence of expansion into the virtual memory subset (Haluszczak et al., 2009), as $>90\%$ of naive GAP50₄₀₋₄₈-specific CD8⁺ T cells expressed low levels of CD44 (Akie et al., 2012). Although the self-derived peptides associated with positive selection of these antigen-specific precursors remain unknown, the uniformly high expression of CD5 by naive GAP50₄₀₋₄₈-specific CD8⁺ T cells suggested the existence of strong TCR-mediated interactions in the thymus (Mandl et al., 2013). It is also notable that V β 8 gene segments are highly represented in laboratory mouse strains (Wilson et al., 2001). High numbers of naive GAP50₄₀₋₄₈-specific CD8⁺ T cells therefore most likely emerged as a consequence of both permissive thymic selection and the frequent generation of V β 8.1⁺ transcripts during the process of somatic recombination. In addition, the presence of a highly conserved V β -D β junction lacking N additions suggested that convergent gene rearrangements, which occur more commonly on a probabilistic basis (Quigley et al., 2010), effectively licensed the extreme penetrance of the V β 8.1 gene-encoded phenotype.

So what are the immunological consequences of such a large pool of antigen-specific precursors in the naive CD8⁺ T cell compartment? Earlier work indicated that CD8⁺ T cells expressing V β 8.1/V β 8.2⁺ TCRs are highly prevalent during malaria infection and contribute to the pathogenesis of ECM (Mariotti-Ferrandiz et al., 2016). In addition, it had been shown previously that high-dose tolerization with the GAP50₄₀₋₄₈ peptide abrogates disease susceptibility in B6 mice (Howland et al., 2013). These observations can be explained by our finding that an

extremely large pool of V β 8.1⁺ antigen-specific naive precursors (~3,000 cells) underpinned the immunodominant CD8⁺ T cell response to GAP50₄₀₋₄₈ and the susceptibility of B6 mice to ECM. In contrast, CB6F1 mice harbored a diminished pool of antigen-specific naive precursors (~1,000 cells), leading to smaller GAP50₄₀₋₄₈-specific CD8⁺ T cell responses and relative resistance to ECM. This causal association was confirmed by the observation that increasing the number of GAP50₄₀₋₄₈-specific CD8⁺ T cells in CB6F1 mice prior to infection rendered them susceptible to ECM. It remains unclear whether similar germline biases can dictate immune responses to malarial antigens in humans, but our data nonetheless provided formal proof of concept that genetic associations with disease outcome can be extended to loci encoding components of the TCR. Moreover, the peak incidence of severe anemia during malaria infection occurs in children under 2 years of age, while cerebral malaria occurs most commonly in children aged 3–5 years who have prior exposure to infection (Struik and Riley, 2004). These epidemiological patterns are consistent with the possibility that larger pre-infection repertoires of malarial antigen-specific T cells predispose to the development of cerebral malaria.

GAP50₄₀₋₄₈-specific memory CD8⁺ T cells are not protective during the liver stage of murine malaria (Doll et al., 2016; Horne-Debets et al., 2016; van der Heyde et al., 1993; Vinetz et al., 1990), and the capacity of CD8⁺ T cells to protect during blood-stage malaria remains controversial (Horne-Debets et al., 2016; Imai et al., 2010; van der Heyde et al., 1993; Vinetz et al., 1990). Thus, the pathogenic effects of GAP50₄₀₋₄₈-specific CD8⁺ T cells in ECM most likely resulted from a large population of precursors, which expanded rapidly after infection to generate substantial numbers of effector cells, leading to sustained immune activation without elimination of the pathogen. In contrast, rapid expansion from the same population of precursors enhanced immune control of primary infection with *L. monocytogenes* expressing the GAP50₄₀₋₄₈ epitope. An unusually large naive CD8⁺ T cell pool can therefore be pathogenic or protective, depending on the nature of the infectious challenge.

In conclusion, we have provided direct evidence that a germline-encoded TCR segment can determine immune responsiveness to an exogenous peptide antigen, thereby extending the concept of *Ir* genes beyond the MHC. The unique features associated with this phenomenon may allow novel interventions to improve vaccine efficacy and limit immune pathology in humans, pending further studies to identify similar genetic associations between disease outcome and heritable components of the TCR.

STAR★METHODS

Detailed methods are provided in the online version of this paper and include the following:

- KEY RESOURCES TABLE
- CONTACT FOR REAGENT AND RESOURCE SHARING
- EXPERIMENTAL MODEL AND SUBJECT DETAILS
- METHOD DETAILS
 - DC-LM immunizations
 - TCR clonotyping
 - Tetramer-based CD8⁺ T cell enrichment
 - Peptide mutants

- Generation of TCR β retrogenic mice
- Isolation of mononuclear cells from the brains of *P. berghei* ANKA-infected mice
- Protein expression, purification, and crystallization
- Data collection and structure determination
- Surface plasmon resonance
- QUANTIFICATION AND STATISTICAL ANALYSIS
- DATA AND SOFTWARE AVAILABILITY

SUPPLEMENTAL INFORMATION

Supplemental Information includes seven figures and six tables and can be found with this article online at <https://doi.org/10.1016/j.immuni.2017.10.013>.

AUTHOR CONTRIBUTIONS

N.V.B.B., S.G., K.L., T.M.J., L.P., S.L.U., C.F., D.A.P., J.R., and J.T.H. designed the study. N.V.B.B., S.G., K.L., T.M.J., L.P., S.L.U., K.L.M., and C.F. conducted experiments. N.V.B.B., S.G., K.L., T.M.J., L.P., S.L.U., K.L.M., C.F., D.A.P., J.R., and J.T.H. analyzed data and interpreted results. N.V.B.B. and S.G. drafted the manuscript. N.V.B.B., S.G., K.L., T.M.J., L.P., S.L.U., C.F., D.A.P., J.R., and J.T.H. edited the manuscript.

ACKNOWLEDGMENTS

We thank Marc Jenkins for helpful discussions, Vladimir Badovinac and Stanley Perlman for constructive comments on the manuscript, Lisa Hancox and Steven Moieffer for excellent technical support, and staff at the New York University Insectary Core and the University of Iowa Flow Cytometry Core. This work was supported by grants from the National Institutes of Health (NIH) (AI42767, AI85515, AI95178, and AI100527 to J.T.H., T32 AI007511 to N.V.B.B., and T32 AI007343 to S.L.U.), the Australian Research Council (ARC) and the Australian National Health and Medical Research Council (NHMRC) to J.R., and the Wellcome Trust to D.A.P. (100326/Z/12/Z). S.G. is a Monash Senior Research Fellow, D.A.P. is a Wellcome Trust Senior Investigator, and J.R. is an ARC Australian Laureate Fellow.

Received: July 5, 2017

Revised: August 2, 2017

Accepted: October 26, 2017

Published: November 14, 2017

REFERENCES

- Akue, A.D., Lee, J.Y., and Jameson, S.C. (2012). Derivation and maintenance of virtual memory CD8 T cells. *J. Immunol.* *188*, 2516–2523.
- Amani, V., Vigário, A.M., Belnoue, E., Marussig, M., Fonseca, L., Mazier, D., and Rénia, L. (2000). Involvement of IFN-gamma receptor-mediated signaling in pathology and anti-malarial immunity induced by *Plasmodium berghei* infection. *Eur. J. Immunol.* *30*, 1646–1655.
- Badovinac, V.P., and Harty, J.T. (2000). Adaptive immunity and enhanced CD8⁺ T cell response to *Listeria monocytogenes* in the absence of perforin and IFN-gamma. *J. Immunol.* *164*, 6444–6452.
- Badovinac, V.P., Messingham, K.A., Jabbari, A., Haring, J.S., and Harty, J.T. (2005). Accelerated CD8⁺ T-cell memory and prime-boost response after dendritic-cell vaccination. *Nat. Med.* *11*, 748–756.
- Behlke, M.A., Chou, H.S., Huppi, K., and Loh, D.Y. (1986). Murine T-cell receptor mutants with deletions of beta-chain variable region genes. *Proc. Natl. Acad. Sci. USA* *83*, 767–771.
- Benacerraf, B. (1974). Editorial: Immune response genes. *Scand. J. Immunol.* *3*, 381–386.
- Benacerraf, B., and Germain, R.N. (1978). The immune response genes of the major histocompatibility complex. *Immunol. Rev.* *38*, 70–119.
- Benacerraf, B., and McDevitt, H.O. (1972). Histocompatibility-linked immune response genes. *Science* *175*, 273–279.

- Bendelac, A., Rivera, M.N., Park, S.H., and Roark, J.H. (1997). Mouse CD1-specific NK1 T cells: development, specificity, and function. *Annu. Rev. Immunol.* **15**, 535–562.
- Bettini, M.L., Bettini, M., Nakayama, M., Guy, C.S., and Vignali, D.A. (2013). Generation of T cell receptor-retrogenic mice: improved retroviral-mediated stem cell gene transfer. *Nat. Protoc.* **8**, 1837–1840.
- Blattman, J.N., Antia, R., Sourdive, D.J., Wang, X., Kaech, S.M., Murali-Krishna, K., Altman, J.D., and Ahmed, R. (2002). Estimating the precursor frequency of naive antigen-specific CD8 T cells. *J. Exp. Med.* **195**, 657–664.
- Boubou, M.I., Collette, A., Voegtli, D., Mazier, D., Cazenave, P.A., and Pied, S. (1999). T cell response in malaria pathogenesis: selective increase in T cells carrying the TCR V(beta)8 during experimental cerebral malaria. *Int. Immunol.* **11**, 1553–1562.
- Brewster, D.R., Kwiatkowski, D., and White, N.J. (1990). Neurological sequelae of cerebral malaria in children. *Lancet* **336**, 1039–1043.
- Busch, D.H., and Pamer, E.G. (1999). T cell affinity maturation by selective expansion during infection. *J. Exp. Med.* **189**, 701–710.
- Busch, D.H., Pilip, I., and Pamer, E.G. (1998). Evolution of a complex T cell receptor repertoire during primary and recall bacterial infection. *J. Exp. Med.* **188**, 61–70.
- Cabaniols, J.P., Fazilleau, N., Casrouge, A., Kourilsky, P., and Kanellopoulos, J.M. (2001). Most alpha/beta T cell receptor diversity is due to terminal deoxynucleotidyl transferase. *J. Exp. Med.* **194**, 1385–1390.
- Chothia, C., Boswell, D.R., and Lesk, A.M. (1988). The outline structure of the T-cell alpha beta receptor. *EMBO J.* **7**, 3745–3755.
- Collaborative Computational Project, Number 4 (1994). The CCP4 suite: programs for protein crystallography. *Acta Crystallogr. D Biol. Crystallogr.* **50**, 760–763.
- Davis, M.M., and Bjorkman, P.J. (1988). T-cell antigen receptor genes and T-cell recognition. *Nature* **334**, 395–402.
- Davis, M.M., Krogsgaard, M., Huppa, J.B., Sumen, C., Purbhoo, M.A., Irvine, D.J., Wu, L.C., and Ehrlich, L. (2003). Dynamics of cell surface molecules during T cell recognition. *Annu. Rev. Biochem.* **72**, 717–742.
- Day, E.B., Guillonneau, C., Gras, S., La Gruta, N.L., Vignali, D.A., Doherty, P.C., Purcell, A.W., Rossjohn, J., and Turner, S.J. (2011). Structural basis for enabling T-cell receptor diversity within biased virus-specific CD8+ T-cell responses. *Proc. Natl. Acad. Sci. USA* **108**, 9536–9541.
- DeLano, W.L. (2002). The PyMOL Molecular Graphics System. <https://pymol.org/2/>.
- Doll, K.L., Pewe, L.L., Kurup, S.P., and Harty, J.T. (2016). Discriminating Protective from Nonprotective Plasmodium-Specific CD8+ T Cell Responses. *J. Immunol.* **196**, 4253–4262.
- Emsley, P., and Cowtan, K. (2004). Coot: model-building tools for molecular graphics. *Acta Crystallogr. D Biol. Crystallogr.* **60**, 2126–2132.
- Engwerda, C., Belnoue, E., Grüner, A.C., and Rénia, L. (2005). Experimental models of cerebral malaria. *Curr. Top. Microbiol. Immunol.* **297**, 103–143.
- Evans, P. (2006). Scaling and assessment of data quality. *Acta Crystallogr. D Biol. Crystallogr.* **62**, 72–82.
- Fulton, R.B., Hamilton, S.E., Xing, Y., Best, J.A., Goldrath, A.W., Hogquist, K.A., and Jameson, S.C. (2015). The TCR's sensitivity to self peptide-MHC dictates the ability of naive CD8(+) T cells to respond to foreign antigens. *Nat. Immunol.* **16**, 107–117.
- Garcia, K.C., Adams, J.J., Feng, D., and Ely, L.K. (2009). The molecular basis of TCR germline bias for MHC is surprisingly simple. *Nat. Immunol.* **10**, 143–147.
- Godfrey, D.I., Uldrich, A.P., McCluskey, J., Rossjohn, J., and Moody, D.B. (2015). The burgeoning family of unconventional T cells. *Nat. Immunol.* **16**, 1114–1123.
- Goldrath, A.W., and Bevan, M.J. (1999). Selecting and maintaining a diverse T-cell repertoire. *Nature* **402**, 255–262.
- Gordon, E.B., Hart, G.T., Tran, T.M., Waisberg, M., Akkaya, M., Kim, A.S., Hamilton, S.E., Pena, M., Yazew, T., Qi, C.F., et al. (2015). Targeting glutamine metabolism rescues mice from late-stage cerebral malaria. *Proc. Natl. Acad. Sci. USA* **112**, 13075–13080.
- Gras, S., Burrows, S.R., Kjer-Nielsen, L., Clements, C.S., Liu, Y.C., Sullivan, L.C., Bell, M.J., Brooks, A.G., Purcell, A.W., McCluskey, J., and Rossjohn, J. (2009). The shaping of T cell receptor recognition by self-tolerance. *Immunity* **30**, 193–203.
- Hafalla, J.C., Bauza, K., Friesen, J., Gonzalez-Aseguinolaza, G., Hill, A.V., and Matuschewski, K. (2013). Identification of targets of CD8+ T cell responses to malaria liver stages by genome-wide epitope profiling. *PLoS Pathog.* **9**, e1003303.
- Haluszczak, C., Akue, A.D., Hamilton, S.E., Johnson, L.D., Pujanauski, L., Teodorovic, L., Jameson, S.C., and Kedl, R.M. (2009). The antigen-specific CD8+ T cell repertoire in unimmunized mice includes memory phenotype cells bearing markers of homeostatic expansion. *J. Exp. Med.* **206**, 435–448.
- Haque, A., Best, S.E., Unosson, K., Amante, F.H., de Labastida, F., Anstey, N.M., Karupiah, G., Smyth, M.J., Heath, W.R., and Engwerda, C.R. (2011). Granzyme B expression by CD8+ T cells is required for the development of experimental cerebral malaria. *J. Immunol.* **186**, 6148–6156.
- Holst, J., Szymczak-Workman, A.L., Vignali, K.M., Burton, A.R., Workman, C.J., and Vignali, D.A. (2006). Generation of T-cell receptor retrogenic mice. *Nat. Protoc.* **1**, 406–417.
- Horne-Debets, J.M., Karunaratne, D.S., Faleiro, R.J., Poh, C.M., Rénia, L., and Wykes, M.N. (2016). Mice lacking Programmed cell death-1 show a role for CD8(+) T cells in long-term immunity against blood-stage malaria. *Sci. Rep.* **6**, 26210.
- Howland, S.W., Poh, C.M., Gun, S.Y., Claser, C., Malleret, B., Shastri, N., Ginhoux, F., Grotenbreg, G.M., and Rénia, L. (2013). Brain microvessel cross-presentation is a hallmark of experimental cerebral malaria. *EMBO Mol. Med.* **5**, 984–999.
- Imai, T., Shen, J., Chou, B., Duan, X., Tu, L., Tetsutani, K., Moriya, C., Ishida, H., Hamano, S., Shimokawa, C., et al. (2010). Involvement of CD8+ T cells in protective immunity against murine blood-stage infection with Plasmodium yoelii 17XL strain. *Eur. J. Immunol.* **40**, 1053–1061.
- Jenkins, M.K., and Moon, J.J. (2012). The role of naive T cell precursor frequency and recruitment in dictating immune response magnitude. *J. Immunol.* **188**, 4135–4140.
- Jerne, N.K. (1971). The somatic generation of immune recognition. *Eur. J. Immunol.* **1**, 1–9.
- Kabsch, W. (2010). XDS. *Acta Crystallogr. D Biol. Crystallogr.* **66**, 125–132.
- Kedl, R.M., Rees, W.A., Hildeman, D.A., Schaefer, B., Mitchell, T., Kappler, J., and Marrack, P. (2000). T cells compete for access to antigen-bearing antigen-presenting cells. *J. Exp. Med.* **192**, 1105–1113.
- Kjer-Nielsen, L., Clements, C.S., Brooks, A.G., Purcell, A.W., McCluskey, J., and Rossjohn, J. (2002). The 1.5 Å crystal structure of a highly selected antiviral T cell receptor provides evidence for a structural basis of immunodominance. *Structure* **10**, 1521–1532.
- Lefranc, M.P. (2003). IMGT databases, web resources and tools for immunoglobulin and T cell receptor sequence analysis. *Leukemia* **17**, 260–266.
- Mach, N., Gillessen, S., Wilson, S.B., Sheehan, C., Mihm, M., and Dranoff, G. (2000). Differences in dendritic cells stimulated in vivo by tumors engineered to secrete granulocyte-macrophage colony-stimulating factor or Flt3-ligand. *Cancer Res.* **60**, 3239–3246.
- Malherbe, L., Hausl, C., Teyton, L., and McHeyzer-Williams, M.G. (2004). Clonal selection of helper T cells is determined by an affinity threshold with no further skewing of TCR binding properties. *Immunity* **21**, 669–679.
- Mandl, J.N., Monteiro, J.P., Vriskoop, N., and Germain, R.N. (2013). T cell-positive selection uses self-ligand binding strength to optimize repertoire recognition of foreign antigens. *Immunity* **38**, 263–274.
- Mariotti-Ferrandiz, E., Pham, H.P., Dulauroy, S., Gorgette, O., Klatzmann, D., Cazenave, P.A., Pied, S., and Six, A. (2016). A TCRβ Repertoire Signature Can Predict Experimental Cerebral Malaria. *PLoS ONE* **11**, e0147871.
- Marshak, A., Doherty, P.C., and Wilson, D.B. (1977). The control of specificity of cytotoxic T lymphocytes by the major histocompatibility complex (AG-B) in rats and identification of a new alloantigen system showing no AG-B restriction. *J. Exp. Med.* **146**, 1773–1790.

- McDevitt, H.O., and Chinitz, A. (1969). Genetic control of the antibody response: relationship between immune response and histocompatibility (H-2) type. *Science* **163**, 1207–1208.
- Miles, J.J., Douek, D.C., and Price, D.A. (2011). Bias in the $\alpha\beta$ T-cell repertoire: implications for disease pathogenesis and vaccination. *Immunol. Cell Biol.* **89**, 375–387.
- Moon, J.J., Chu, H.H., Pepper, M., McSorley, S.J., Jameson, S.C., Kedl, R.M., and Jenkins, M.K. (2007). Naive CD4(+) T cell frequency varies for different epitopes and predicts repertoire diversity and response magnitude. *Immunity* **27**, 203–213.
- Neller, M.A., Ladell, K., McLaren, J.E., Matthews, K.K., Gostick, E., Pentier, J.M., Dolton, G., Schauenburg, A.J., Koning, D., Fontaine Costa, A.I., et al. (2015). Naive CD8⁺ T-cell precursors display structured TCR repertoires and composite antigen-driven selection dynamics. *Immunol. Cell Biol.* **93**, 625–633.
- Obar, J.J., Khanna, K.M., and Lefrançois, L. (2008). Endogenous naive CD8+ T cell precursor frequency regulates primary and memory responses to infection. *Immunity* **28**, 859–869.
- Owens, T., and Zeine, R. (1989). The cell biology of T-dependent B cell activation. *Biochem. Cell Biol.* **67**, 481–489.
- Pham, N.L., Badovinac, V.P., and Harty, J.T. (2009). A default pathway of memory CD8 T cell differentiation after dendritic cell immunization is deflected by encounter with inflammatory cytokines during antigen-driven proliferation. *J. Immunol.* **183**, 2337–2348.
- Price, D.A., Brenchley, J.M., Ruff, L.E., Betts, M.R., Hill, B.J., Roederer, M., Koup, R.A., Migueles, S.A., Gostick, E., Wooldridge, L., et al. (2005). Avidity for antigen shapes clonal dominance in CD8+ T cell populations specific for persistent DNA viruses. *J. Exp. Med.* **202**, 1349–1361.
- Quigley, M.F., Greenaway, H.Y., Venturi, V., Lindsay, R., Quinn, K.M., Seder, R.A., Douek, D.C., Davenport, M.P., and Price, D.A. (2010). Convergent recombination shapes the clonotypic landscape of the naive T-cell repertoire. *Proc. Natl. Acad. Sci. USA* **107**, 19414–19419.
- Quigley, M.F., Almeida, J.R., Price, D.A., and Douek, D.C. (2011). Unbiased molecular analysis of T cell receptor expression using template-switch anchored RT-PCR. *Curr. Protoc. Immunol.* **10**, 33.1–33.16.
- Rai, D., Pham, N.L., Harty, J.T., and Badovinac, V.P. (2009). Tracking the total CD8 T cell response to infection reveals substantial discordance in magnitude and kinetics between inbred and outbred hosts. *J. Immunol.* **183**, 7672–7681.
- Read, R.J. (2001). Pushing the boundaries of molecular replacement with maximum likelihood. *Acta Crystallogr. D Biol. Crystallogr.* **57**, 1373–1382.
- Rossjohn, J., Gras, S., Miles, J.J., Turner, S.J., Godfrey, D.I., and McCluskey, J. (2015). T cell antigen receptor recognition of antigen-presenting molecules. *Annu. Rev. Immunol.* **33**, 169–200.
- Savage, P.A., Boniface, J.J., and Davis, M.M. (1999). A kinetic basis for T cell receptor repertoire selection during an immune response. *Immunity* **10**, 485–492.
- Scott-Browne, J.P., White, J., Kappler, J.W., Gapin, L., and Marrack, P. (2009). Germline-encoded amino acids in the alpha beta T-cell receptor control thymic selection. *Nature* **458**, 1043–1046.
- Struik, S.S., and Riley, E.M. (2004). Does malaria suffer from lack of memory? *Immunol. Rev.* **201**, 268–290.
- Townsend, A.R., Gotch, F.M., and Davey, J. (1985). Cytotoxic T cells recognize fragments of the influenza nucleoprotein. *Cell* **42**, 457–467.
- Turner, S.J., Doherty, P.C., McCluskey, J., and Rossjohn, J. (2006). Structural determinants of T-cell receptor bias in immunity. *Nat. Rev. Immunol.* **6**, 883–894.
- Valkenburg, S.A., Quiñones-Parra, S., Gras, S., Komadina, N., McVernon, J., Wang, Z., Halim, H., Iannello, P., Cole, C., Laurie, K., et al. (2013). Acute emergence and reversion of influenza A virus quasispecies within CD8+ T cell antigenic peptides. *Nat. Commun.* **4**, 2663.
- van der Heyde, H.C., Manning, D.D., Roopenian, D.C., and Weidanz, W.P. (1993). Resolution of blood-stage malarial infections in CD8+ cell-deficient beta 2-m/0 mice. *J. Immunol.* **151**, 3187–3191.
- van der Merwe, P.A., and Dushek, O. (2011). Mechanisms for T cell receptor triggering. *Nat. Rev. Immunol.* **11**, 47–55.
- Van Rhijn, I., Godfrey, D.I., Rossjohn, J., and Moody, D.B. (2015). Lipid and small-molecule display by CD1 and MR1. *Nat. Rev. Immunol.* **15**, 643–654.
- Vinetz, J.M., Kumar, S., Good, M.F., Fowlkes, B.J., Berzofsky, J.A., and Miller, L.H. (1990). Adoptive transfer of CD8+ T cells from immune animals does not transfer immunity to blood stage Plasmodium yoelii malaria. *J. Immunol.* **144**, 1069–1074.
- Wilson, A., Maréchal, C., and MacDonald, H.R. (2001). Biased V beta usage in immature thymocytes is independent of DJ beta proximity and pT alpha pairing. *J. Immunol.* **166**, 51–57.
- Yañez, D.M., Manning, D.D., Cooley, A.J., Weidanz, W.P., and van der Heyde, H.C. (1996). Participation of lymphocyte subpopulations in the pathogenesis of experimental murine cerebral malaria. *J. Immunol.* **157**, 1620–1624.
- Young, A.C., Zhang, W., Sacchettini, J.C., and Nathenson, S.G. (1994). The three-dimensional structure of H-2Db at 2.4 Å resolution: implications for antigen-determinant selection. *Cell* **76**, 39–50.
- Zhao, J., Zhao, J., and Perlman, S. (2009). De novo recruitment of antigen-experienced and naive T cells contributes to the long-term maintenance of antiviral T cell populations in the persistently infected central nervous system. *J. Immunol.* **183**, 5163–5170.
- Zinkernagel, R.M. (1978). Thymus and lymphohemopoietic cells: their role in T cell maturation in selection of T cells' H-2-restriction-specificity and in H-2 linked Ir gene control. *Immunol. Rev.* **42**, 224–270.